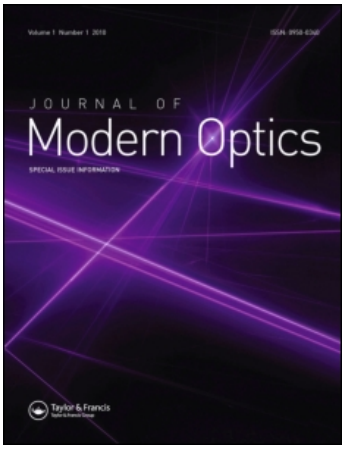

Journal of Modern Optics
Publication details, including instructions for authors and subscription information:
http://www.informaworld.com/smpp/title~content=t713191304

Two-photon ionization of atoms by ultrashort laser pulses

Kenichi L. Ishikawa[a]; Yohei Kawazura[b]; Kiyoshi Ueda[c]
[a] Computational Science Research Program, Wako, Japan [b] Graduate School of Frontier Sciences, The University of Tokyo, Kashiwa, Japan [c] Institute of Multidisciplinary Research for Advanced Materials, Tohoku University, Sendai, Japan

First published on: 17 December 2009

To cite this Article Ishikawa, Kenichi L. , Kawazura, Yohei and Ueda, Kiyoshi(2010) 'Two-photon ionization of atoms by ultrashort laser pulses', Journal of Modern Optics, 57: 11, 999 — 1007, First published on: 17 December 2009 (iFirst)
To link to this Article: DOI: 10.1080/09500340903511703
URL: http://dx.doi.org/10.1080/09500340903511703

Journal of Modern Optics
Vol. 57, No. 11, 20 June 2010, 999–1007

Taylor & Francis
Taylor & Francis Group

Two-photon ionization of atoms by ultrashort laser pulses

Kenichi L. Ishikawa[a]*†, Yohei Kawazura[b] and Kiyoshi Ueda[c]

[a]*Computational Science Research Program, RIKEN, Wako, Japan;* [b]*Graduate School of Frontier Sciences, The University of Tokyo, Kashiwa, Japan;* [c]*Institute of Multidisciplinary Research for Advanced Materials, Tohoku University, Sendai, Japan*

(*Received 30 July 2009; final version received 23 November 2009*)

Based on the direct solution of the time-dependent Schrödinger equation (TDSE), we theoretically study two-photon ionization (TPI) of a hydrogen atom by ultrashort vacuum ultraviolet (VUV) laser pulses with a photon energy close to the ionization threshold and a pulse width from 10 fs down to subfemtoseconds, for which the distinction between stepwise and direct processes becomes subtle. Our analysis on TPI by a double pulse reveals that direct processes are classified into two categories: a purely direct process with no real intermediate levels, and the one via Rydberg or continuum states, which rapidly escape from the nucleus. Our results also show that TPI becomes stepwise for subfemtosecond VUV pulses even for a wavelength corresponding to a direct process in the long pulse limit, since the broad spectrum of the pulse overlaps several discrete bound levels and excites them resonantly. This also leads to a phenomenon peculiar to attosecond pulses, namely, a significant red shift of the photoelectron energy spectrum. The Rydberg wave packet generated by an ultrashort near-threshold laser pulse, containing low-lying levels and the continuum, rapidly disintegrates into several parts. Nevertheless, the bound parts come back to the nucleus in fragments, and each fragment returns in the Kepler orbit time corresponding to its central principal quantum number. The lower-energy part of the double-pulse TPI electron energy spectrum exhibits the effect of the interference between the returning fragments and the wave packet excited by the second pulse.

Keywords: two-photon ionization; Rydberg wave packet; time-dependent Schrödinger equation

1. Introduction

The recent progress in the high-order harmonic generation (HHG) technique [1–4] has enabled the development of new soft X-ray sources with two distinct characteristics. On one hand, ultrashort pulses with a duration down to 80 attoseconds [5] can now reveal ultrafast motion of electrons inside an atom [6–9] and are applied to direct measurement of light waves [10]. On the other hand, high-power pulses produced with a phase-matching technique [11–17] can induce multi-photon ionization [18–22]. Sekikawa et al. [18] have characterized extreme ultraviolet pulses (photon energy 27.9 eV) with a pulse duration of 950 as by an autocorrelation technique, based on two-photon above-threshold ionization of helium. Hasegawa et al. [19] have recently observed two-photon double ionization of helium by Ti:sapphire 27th harmonic pulses (photon energy 41.8 eV), and this has been applied to the autocorrelation measurement of the pulse duration of the soft X-ray pulses [23].

This progress has triggered an increasing number of theoretical studies on two-photon double ionization (TPDI) of He by ultrashort soft X-ray pulses [24–33]. Recently, Ishikawa and Midorikawa [26] have investigated TPDI of He by ultrashort pulses with a photon energy of 91.45 eV and pulse durations of 150–450 as pertinent to HHG sources, based on direct solution of the two-electron time-dependent Schrödinger equation. They have identified an 'anomalous' component in the electron spectrum between the two peaks, associated with sequential double ionization, and explained its origin in terms of second ionization during core relaxation. This has evoked discussion on the sequentiality of ionization in the ultrashort pulse regime. Barna et al. [27] and Foumouo et al. [28] have argued that the notion of sequentiality of ionization events loses its meaning in the case of attosecond pulses.

Analogous to sequential and non-sequential two-photon double ionization, two-photon *single* ionization of atoms may be classified into two categories in general: stepwise and direct. A naive criterion to distinguish between the two, valid in the limit of long pulse, would be that electrons are ejected via a real intermediate level in the former and not in the latter. This may, however, become obscure for the case of

*Corresponding author. Email: ishiken@atto.t.u-tokyo.ac.jp
† Present address: Photon Science Center, Graduate School of Engineering, the University of Tokyo, Tokyo, Japan

ISSN 0950–0340 print/ISSN 1362–3044 online

DOI: 10.1080/09500340903511703
http://www.informaworld.com

ultrashort intense laser pulses in two senses. First, even though the central wavelength is not resonant with any level, a part of the spectrum that is broadened due to ultrashort pulse length can overlap one or several levels. Second, above-threshold ionization (ATI) due to high intensity, in which outgoing photoelectrons absorb further photons than the minimum necessary for ionization, is usually regarded as direct in spite of the fact that it proceeds via real intermediate continuum states.

In the present work, we theoretically study two-photon ionization of a hydrogen atom by ultrashort vacuum ultraviolet laser pulses with a pulse width from subfemtosecond to, at most, 10 fs. Although the study on the TPI of a hydrogenlike atom has a long history and the cross-section is tabulated or graphed in the literature [34–39], these values are valid only at the long-pulse limit, strictly speaking. On the other hand, there is little work for ultrashort pulses [40]. In particular, in this article, we focus on how the TPI yield and photoelectron energy spectra changes with decreasing pulse width, and on how the TPI proceeds in the ultrashort pulse regime, topics that have not been studied systematically before, to our knowledge. We solve numerically the time-dependent Schrödinger equation for H interacting with an ultrashort laser pulse using the alternating direction implicit method [41], and obtain the ionization yield and electron energy spectra.

We first analyze the ratio of the TPI yield by a double pulse to that by a single pulse with a duration of 10 fs. Our results show that there are two classes of 'direct' TPI: the case where there is no resonant intermediate level, and the case where the Rydberg or continuum wave packet escapes immediately. In such cases, although the ionization yield linearly depends on pulse width for the case of long pulses, the linear relation breaks down for a pulse shorter than ca. 1 fs, containing only a few optical cycles, since the pulse spectrum is so broad that several discrete bound levels can be resonantly excited, regardless of the central wavelength. This also leads not only to broadening but also to a significant shift of the electron energy spectrum, a phenomenon peculiar to attosecond pulses.

We also investigate the evolution of the wave packet generated by an ultrashort laser pulse whose photon energy is slightly smaller than ionization potential. Similar situations are encountered if one irradiates a He atom with an attosecond high harmonic pulse generated from Xe. In the picosecond regime, it has long been known that when a short pulse is used to excite an atom to high-lying Rydberg levels, many levels are simultaneously and coherently excited to form a Rydberg wave packet, which is well localized in space and can come back to the nucleus in the classical Kepler orbit time. The returning wave packet could be detected, for example, by inducing transition to another (bound) level [42]. It has also shown that the influence of the relative phase of the two pulses on the total population of the wave packet can be seen as Ramsey fringes [43,44]. On the other hand, in the ultrashort pulse regime considered in the present study, the spectral bandwidth is so broad, spanning even up to the continuum, that the wave packet disintegrates [45] before the Kepler orbit time. Nevertheless, it is considered that the wave packet evolution itself is coherent and that the disintegrated wave packet returns to the nucleus by fragments. Our results show that the lower-energy part of the double-pulse TPI electron energy spectrum exhibits the effect of the interference between the returning fragments and the wave packet excited by the second pulse, depending on the pulse delay.

The present paper is organized as follows. Section 2 summarizes the simulation model. In Section 3 we apply the model to the calculation of two-photon ionization of a hydrogen atom by a double pulse and examine the difference between a stepwise and direct process in terms of the ratio of the yield to that by a single pulse. We investigate, in Section 4, how the TPI of a hydrogen atom depends on the pulse width in case of extremely short pulse of only a few optical cycles. In Section 5 we examine the evolution of the Rydberg wave packet excited by an ultrashort laser pulse. The conclusions are given in Section 6.

2. Model

To study the interaction of a hydrogen atom initially in the ground state with a laser pulse, we numerically solve the one-electron TDSE in the length gauge,

$$i\frac{\partial\Phi(\mathbf{r},t)}{\partial t}=\left[-\frac{1}{2}\nabla^2-\frac{1}{r}+zE(t)\right]\Phi(r,t), \qquad (1)$$

where $E(t)$ is the electric field of the pulse. Here we have assumed that the field is linearly polarized in the z-direction. Equation (1) is numerically integrated using the alternating direction implicit (Peaceman–Rachford) method [41]. The numerical scheme is now well documented [41,46] and not difficult to implement. The ionization yield is evaluated as the decrease of the norm of the wave function on the grid, or equivalently, the number of electrons absorbed by the mask function. In typical calculations, we use a grid with a maximum radius of 5000 a.u. and maximum number of partial waves $L_{\max}=3$. The grid spacing is 0.25 a.u., and the time step is 1/1024 of an optical cycle t_L of the laser light with a wavelength of 800 nm.

The photoelectron spectra are determined with the help of a spectral analysis of the atomic wave function, as obtained immediately after the pulse. We used the technique developed in [47], which is based on the use of the window operator:

$$W(E_k, \gamma) = \frac{\gamma^4}{(H_{\rm at} - E_k)^4 + \gamma^4}, \tag{2}$$

where $\gamma = 0.1\,\text{eV}$ (in our case) indicates the energy resolution of our analysis. We then defined the photoelectron spectra as $P(E_k) = \langle \Phi | W(E_k, \gamma) | \Phi \rangle$.

3. Two-photon ionization of H by double pulse

In this section, we examine two-photon ionization of a hydrogen atom by an ultrashort double pulse, in terms of the difference between stepwise and direct ionization. For direct TPI, we expect that the yield by a double pulse is twice as much as by a single pulse, as long as the depletion of the ground state remains negligible. The thick solid lines in Figure 1 show the calculated energy spectra of an electron ejected by a double pulse whose temporal profile is given by,

$$E(t) = E_s(t) + E_s(t - \tau), \tag{3}$$

where τ is the time delay between the pulses, and each single pulse has a Gaussian temporal profile $E_s(t)$:

$$E_s(t) = E_0 \exp\left[-\frac{(2\ln 2)\, t^2}{T^2}\right] \cos \omega t, \tag{4}$$

where E_0 denotes the peak field amplitude, T the full width at half maximum (FWHM) of the pulse duration, and ω the angular frequency. The pulse peak is taken as the origin of time t. For Figure 1 we have used $\tau = 64.04\,\text{fs}$, $T = 10\,\text{fs}$, and the value of E_0 corresponding to a peak intensity I of $10^{13}\,\text{W/cm}^2$, for which three-photon ATI is negligible. The thin solid lines in Figure 1 show the electron energy spectra by a single pulse whose temporal profile is given by $E(t) = E_s(t)$.

Let us denote the ratio of the ionization yield by a double pulse to that by a single pulse as η. For the case of $\hbar\omega = 12.5\,\text{eV}$, there is no resonant intermediate level; the TPI is purely direct, and the first and second pulses act independently from each other. Thus, the ratio η is equal to 2. On the other hand, for $\hbar\omega = 13\,\text{eV}$, η is much larger than 2. This reflects the fact that the photon energy is nearly resonant with the $1s$–$5p$ transition (13.06 eV). The electron is lifted to the continuum via the $5p$ level in a stepwise manner, and the level is still populated when the second pulse arrives. In such a case, the ratio η differs from 2 in general, and is an oscillating function of the delay τ_d or the relative phase $\phi_{\rm rel}$ between the first and the second pulse, as is shown in Figure 2. In the limit of weak and long pulses and if we assume Gaussian pulses are exactly resonant with an intermediate level, it is not difficult to show that η oscillates between the values 8.58 for constructive interference and 2 for destructive interference. The apparent discrepancy from this found in Figure 2 can be attributed to the ultrashortness and high intensity of the pulses: the pulse populates not only the $5p$ level but also other states due to the broad spectrum, and high intensity leads to significant depletion ($\approx$27% after the first pulse) of the ground state.

Let us now turn to the case where the photon energy $\hbar\omega$ is close to the ionization threshold $I_p = 13.605\,\text{eV}$. Single photon absorption can lift the electron to the continuum if $\hbar\omega > I_p$ and excite a Rydberg wave packet if $\hbar\omega < I_p$. In either case, the TPI

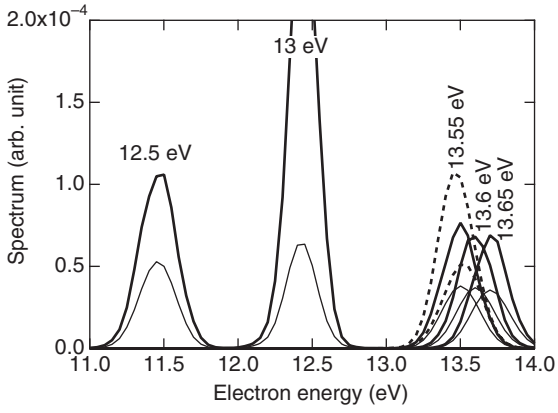

Figure 1. Electron energy spectra resulting from the TPI of H by a 10 fs single (thin solid line) and double (thick solid line) with a photon energy $\hbar\omega$ indicated in the figure. The pulse delay τ for the double pulse is 64.04 fs.

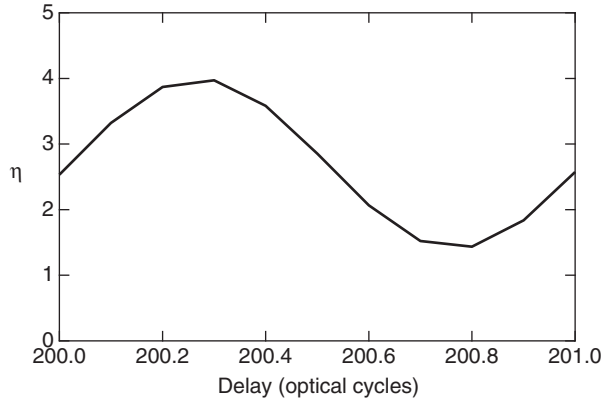

Figure 2. Oscillation of the ratio η of the ionization yield by double pulse to that by a single pulse as a function of the delay of the second pulse for the case of $\hbar\omega = 13\,\text{eV}$ and $T = 10\,\text{fs}$.

proceeds via real intermediate states. This argument alone would seem to indicate that the TPI is a stepwise process. However, the (Rydberg or continuum) p states populated by the first pulse do not contribute to stepwise TPI, since the generated wave packet rapidly escapes from the nucleus, as we will see in Section 5, before the arrival of the second pulse. As a consequence, the double-to-single pulse ratio η behaves much as the case of $\hbar\omega = 12.5\,\text{eV}$, i.e. $\eta(=2)$ does not depend on τ_d, and the ATI would be observed as a direct process despite intermediate level excitation. It should also be noted that the continuous transition from below- (13.55 eV) to above-threshold (13.65 eV) TPI seen in Figure 1 reflects continuity of the oscillator strength spectral density across the ionization threshold [48].

It follows from the above discussion that, when we mention 'direct' TPI, it contains two different classes. First, a purely direct process with no real intermediate states involved, and second, a process involving Rydberg or continuum states as an intermediate level whose escaping time is, however, very short. It should be noted that the presence of an intermediate resonant level, even bound, does not mean that the TPI is stepwise.

4. Two-photon ionization by an extremely short pulse

The discussion in the previous section may raise a naive question: does TPI behave as stepwise if the pulse delay τ is so short that the wave packet generated by single-photon absorption remains in the vicinity of the nucleus when the second pulse arrives? The pulse delay, however, cannot be shorter than the pulse width. Therefore, it is more convenient to examine, instead, how the TPI by a single pulse depends on its pulse width. As is discussed in [26], we would expect linear and quadratic dependence of the TPI yield on T for a direct and stepwise process, respectively. Then the question in the beginning of this section reads as: does the dependence tend to be quadratic as the pulse becomes ultrashort?

Figure 3(a) presents the TPI yield by a single pulse with a photon energy of 13.65 eV and a peak intensity I of $10^{13}\,\text{W/cm}^2$ as a function of its pulse width. The field of the pulse is given by Equation (4). Note that one optical cycle corresponds to 0.3 fs. In Figure 3(a), we see that the linear relation approximately holds at $T > 1$ fs. In this region, the TPI is dominated by a direct process. On the other hand, the linearity breaks down for shorter pulses. The dependence is, however, not quadratic, either. In order to explore the origin of this behavior, we show the energy spectrum of the electron with an angular momentum $l = 1$ after the pulse for several different values of pulse width in Figure 4. The apparent finite width of bound levels ($\approx$0.2 eV) stems from the window width γ in Equation (2). This figure indicates that the uncertainty principle leads to the spectral broadening of the pulse (FWHM of 1.8, 2.3,

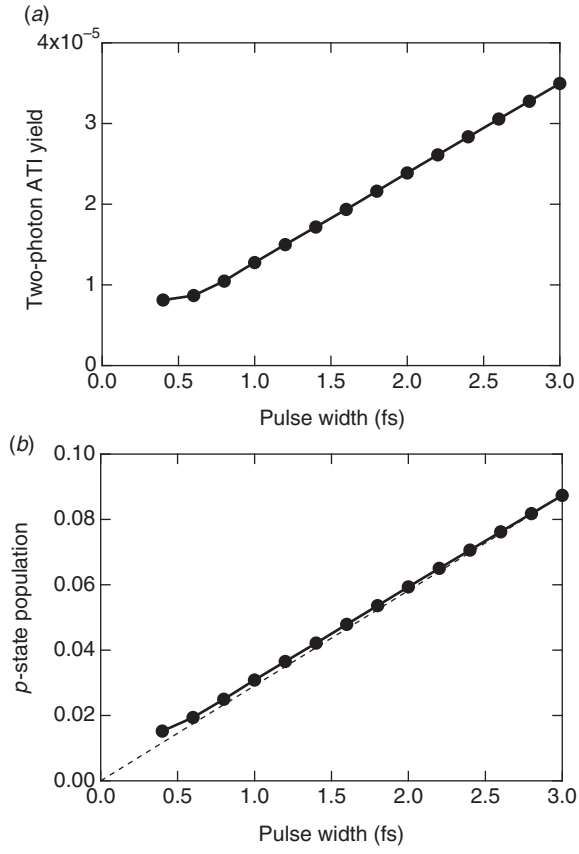

Figure 3. (a) TPI yield by a single pulse with a photon energy of 13.65 eV and a peak intensity of $10^{13}\,\text{W/cm}^2$ as a function of its pulse width. (b) The p-state population after the pulse as a function of pulse width under the same condition.

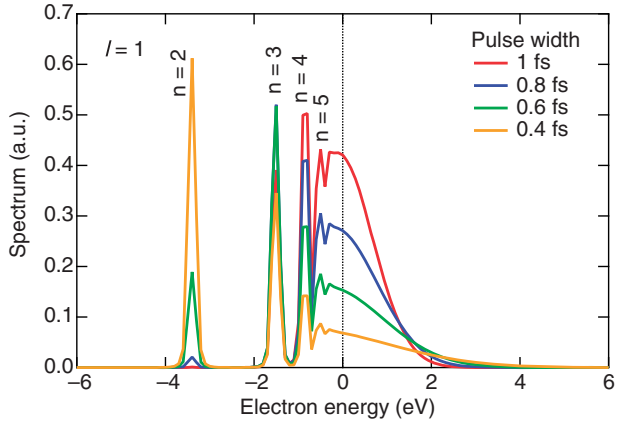

Figure 4. Energy spectrum of the p-state electron after the pulse with a photon energy of 13.65 eV and several different values of pulse width. (The color version of this figure is included in the online version of the journal.)

3.0, 4.6 eV for 1, 0.8, 0.6, 0.4 fs pulsewidths, respectively) and to resonant excitation of different discrete bound levels. The $3p$ level (-1.5 eV) is most populated around $T = 0.6$ fs, and the pulse with $T = 0.4$ fs populates the $2p$ level (-3.4 eV) more efficiently than longer pulses containing more photons in total.

The single photon absorption yield Y, i.e. p-state population after the pulse, is given by

$$Y = \int \sigma(\omega) W(\omega) \mathrm{d}\omega = \int \sigma(\omega) \frac{I(\omega) T}{\hbar\omega} \mathrm{d}\omega, \qquad (5)$$

with $\sigma(\omega)$ and $W(\omega)$ being the cross-section and the photon fluence, respectively, for frequency ω, and $I(\omega)$ denotes intensity spectrum. We show the p-state population Y as a function of pulse width T in Figure 3(b). The population deviates upward as the pulse width becomes shorter. This trend can be explained as follows. $\sigma(\omega)$ is proportional to oscillator strength $df/d\omega$. For the case of a hydrogen atom, $df/d\omega$, and thus $\sigma(\omega)/\hbar\omega$, is a decreasing convex function of ω as can be found in Figure 1(a) of [48], in which the strengths of discrete transitions are also included in the form of a histogram. In consequence, since the intensity spectrum $I(\omega)$ is broader for a smaller value of T, the ratio Y/T increases as T decreases, as can be seen from Figure 3(b). In addition, for a given photon energy $\hbar\omega$, the coupling with the continuum is stronger for lower bound states. Hence, the TPI yield deviates upward from a linear relationship with pulse width, as we have seen in Figure 3(a).

In the extremely short pulse regime shorter than 1 fs, the pulse populates low-lying bound levels due to spectral broadening, although the central photon energy is larger than the ionization potential. In this sense, therefore, the TPI is of stepwise nature, as we speculated at the beginning of the present section. Against our expectation, however, the yield does not depend quadratically on pulse width T, since the spectral broadening and the relative population of different bound levels strongly depend on T.

The two-photon ATI yield is much smaller than the p-state population in Figure 3. Thus, the interaction is still in the perturbative regime at a relatively high intensity of 10^{13} W/cm^2. This is supported by the fact that the Keldysh parameter $\gamma_K \equiv \sqrt{2\omega^2 I_p / I} \approx 30$ is much larger than unity, and is also confirmed by Figure 5, which shows that the d- and p-state populations depend quadratically and linearly on peak intensity I, respectively.

The excitation of low-lying bound levels and the importance of the contribution of the lower-energy part in the spectrum to TPI have a remarkable effect peculiar to attosecond pulses on the TPI electron energy spectra. Figure 6(a) exhibits TPI electron energy spectra for different values of pulse width T. It should be noted that the peak position for sub-fs pulses is significantly shifted to lower energy from the value in the long pulse limit (13.7 eV). This is in marked contrast to the case of a single-photon ionization (Figure 6(b)), for which the peak shift is much less significant. While different features that appear when one uses attosecond pulses have also been predicted in the energy- and angular distribution of TPDI photoelectrons [24–28,30–33], it is noteworthy that an effect of attosecond pulses manifests itself in such a simple observable.

5. Dynamics of Rydberg wave packets

In the picosecond regime, it has long been known that when a short pulse is used to excite an atom to high-lying Rydberg levels, many levels are simultaneously and coherently excited to form a Rydberg wave packet, which is well localized in space and can come back to the nucleus. It is theoretically predicted

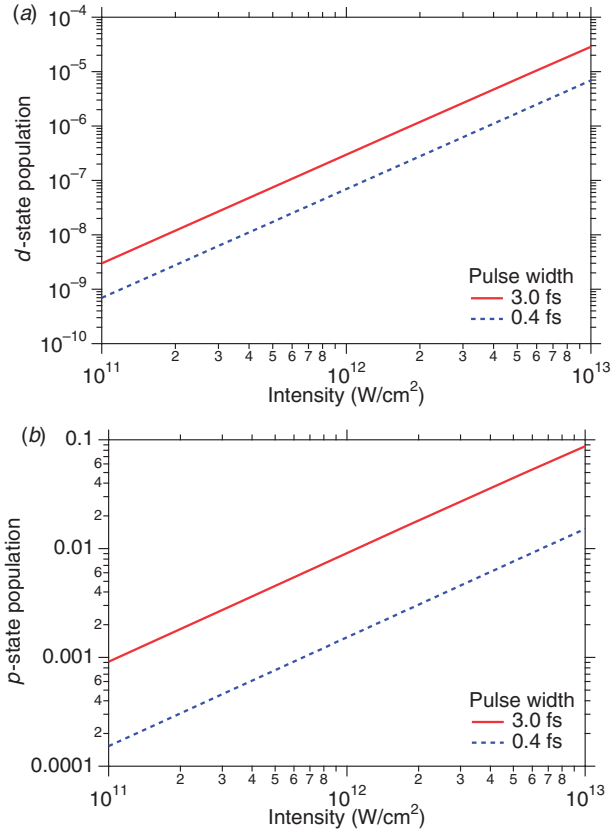

Figure 5. (a) The d-state population after a single pulse with a photon energy of 13.65 eV and a pulse width of 0.4 and 3.0 fs as a function of peak intensity. (b) The p-state population after the pulse as a function of peak intensity under the same condition. (The color version of this figure is included in the online version of the journal.)

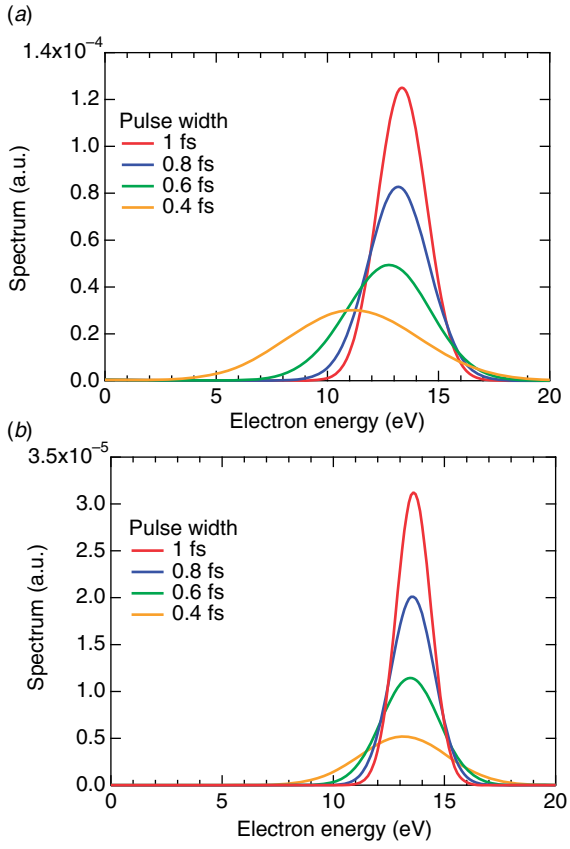

Figure 6. (*a*) Energy spectra of the electrons ejected through TPI by a pulse with a photon energy of 13.65 eV, a peak intensity of 10^{13} W/cm^2, and different values of pulse width. (*b*) Energy spectra of the electrons ejected through single photon ionization by a pulse with a photon energy of 27.3 eV, a peak intensity of 10^{10} W/cm^2, and different values of pulse width. (The color version of this figure is included in the online version of the journal.)

[42] that in a time-delayed two-photon experiment, where the first laser pulse generates a wave packet, which is then probed by a second short pulse, the two-photon transition probability shows peaks when the time delay is a multiple of the classical Kepler orbit time,

$$\tau_n = 2\pi n^3. \tag{6}$$

In fact, Wolde et al. [49] have observed returning wave packets of rubidium atoms around $n = 41$ in a direct pump-probe experiment with 6 ps laser pulses. In this section, we discuss how Rydberg wave packets excited by ultrashort laser pulses as considered in the present work evolve in time.

Figure 7 displays the temporal evolution of the p wave population at $r < 50$ a.u. when an hydrogen atom is subject to a 10 fs pulse with $\hbar\omega = 13.55$ eV and a peak intensity of 10^{13} W/cm^2. Since the 10 fs pulse width translates to a spectral width of 0.18 eV, the excited

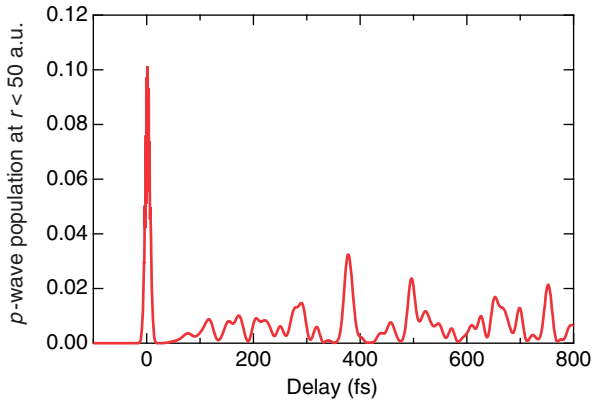

Figure 7. Temporal evolution of the population at $r < 50$ a.u. of the p-wave packet generated by the first pulse with $T = 10$ fs and $\hbar\omega = 13.55$ eV (the second pulse in Equation (3) is suppressed). (The color version of this figure is included in the online version of the journal.)

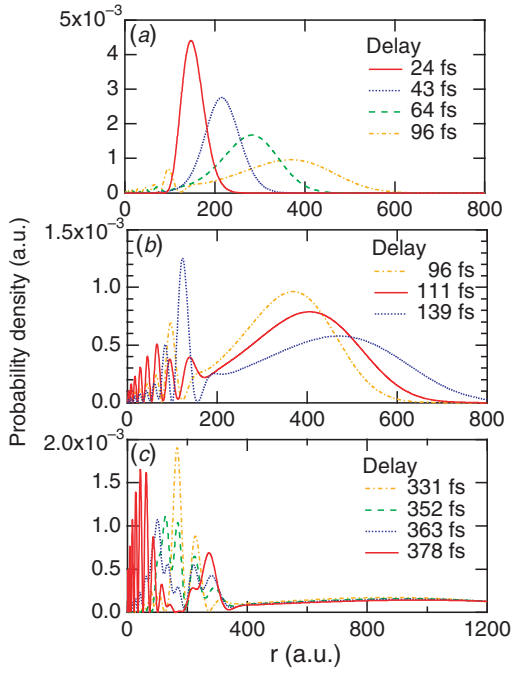

Figure 8. Radial probability density distribution of the p-wave packet generated by the first pulse with $T = 10$ fs and $\hbar\omega = 13.55$ eV (the second pulse in Equation (3) is suppressed) at different time delays τ, indicated in each panel. (The color version of this figure is included in the online version of the journal.)

wave packet has a broad spectrum centered at $n = 16$ but spanning approximately from $n = 8$ even to the continuum. As a consequence, the wave packet is not so well localized radially as in the case of picosecond laser pulses [42], but disintegrates [45] before the Kepler orbit time. Figure 8 illustrates the radial

Table 1. Energy eigenvalue and the Kepler orbit time τ_n calculated from Equation (6) for several values of principal quantum number n.

n	Energy (eV)	τ_n (fs)
8	−0.213	78
9	−0.168	111
10	−0.136	152
11	−0.112	202
12	−0.094	263
13	−0.081	334
14	−0.069	417
15	−0.060	513
16	−0.053	622
17	−0.047	747

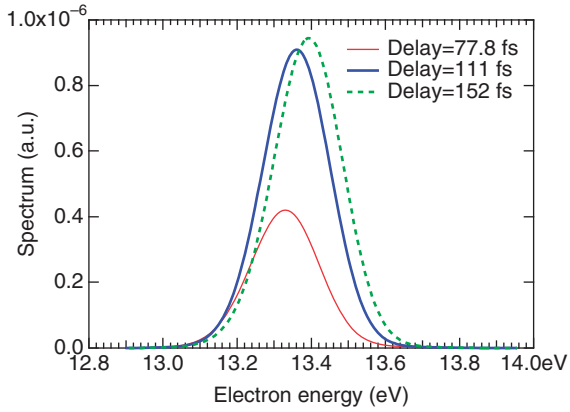

Figure 9. Energy spectra of electrons ejected by the second pulse at three different values of time delay τ indicated in the figure, corresponding to 255, 364, and 498 optical cycles, respectively. The peak intensity of the second pulse is set 1000 times weaker than that of the first pulse, to suppress direct two photon ionization from the ground state and to extract only the stepwise contribution from the wave packet formed by the first pulse. (The color version of this figure is included in the online version of the journal.)

distribution of the wave packet at various delay times after its generation by the first pulse. The initially well localized wave packet moves outward and spreads rapidly. Already at $\tau = 64$ fs, the inner part of the packet begins to be dispersed by the strong Coulomb potential [45] (Figure 8(*a*)). At later time in Figure 8(*b*), the wave packet gets separated more clearly into two parts. At the outer region at $r > 160$ a.u., a broad but well-formed wave packet moves outward and spreads further. This part contains a population in high-lying Rydberg and continuum states. On the other hand, we can see that the inner part bound at $r < 160$ a.u. oscillates as time passes from $\tau = 96$ fs to 139 fs. At an even later time in Figure 8(*c*), a knee-like structure around $r = 310$ a.u. at $\tau = 331$ fs separates from the outgoing part, returns toward the nucleus, and forms a well-shaped Rydberg part for a while as can be seen at 160 a.u. $< r < 340$ a.u. for $\tau = 378$ fs. Thus, the wave packet disintegrates into several parts and returns to the nucleus in fragments with different time delays, as can be seen in Figure 7.

The values of the Kepler orbit time τ_n naively calculated with Equation (6) for relatively small values of n are listed in Table 1. These do correspond to first several peaks in Figure 7. For example, it seems that small peaks situated at 77, 116, 154, 205, 500, 626, and 752 fs correspond to the return of wave packets centered at $n = 8$, 9, 10, 11, 15, 16 and 17, respectively. To reinforce this speculation, we have performed the following thought experiment. Figure 9 shows the energy spectra of electrons ejected by the second pulse with $\tau = 77.8$ fs (255 optical cycles), 111 fs (364 optical cycles), and 152 fs (498 optical cycles). We have performed simulations for a peak intensity of the second pulse of 10^{10} W/cm^2, which is 1000 times lower than the first pulse, in order to suppress direct two-photon ionization from the ground state. The peak position is 13.33 eV for $\tau = 77.8$ fs, 13.36 eV for $\tau = 111$ fs, and 13.40 eV for $\tau = 152$ fs, which are close to the theoretical values, 13.34 eV for $n = 8$, 13.38 eV for $n = 9$, and 13.41 eV for $n = 10$. This indicates that even in the case of ultrashort laser pulses, for which the wave packet disintegrates rapidly, each fragment returns to the nucleus in the Kepler orbit time corresponding to its own central value of n, at least, in the early stages. Although in actual experiments the spectrum by the second pulse as in Figure 9 would interfere with that by the first pulse, the contributions from the first and second pulses could be distinguished from each other in principle by streaking the latter with a terahertz pulse, which is an idea analogous to attosecond double-slit experiments [50,51].

A relatively large peak is present at the delay $\tau = 378$ fs, which corresponds to the Kepler orbit time for $n = 13.5$. As can be seen from the bottom panel of Figure 8, at this time the wave packet is separated roughly into three parts; the inner dispersed part at $r < 160$ a.u., the well-formed Rydberg part at 160 a.u. $< r < 340$ a.u., and, in addition, the outer continuum part at $r > 340$ a.u.

We have performed simulations for a sequence of two equivalent pulses whose field is of the form Equation (3), by varying τ between 1237 and 1238 optical cycles ($\tau \approx 378$ fs) in such a way that $\phi_{\rm rel}$ changes from 0 to 2π. In Figure 10 we show the electron energy spectrum. If we compare the spectra for $\phi_{\rm rel} = 0$ ($\pi/2$) and π ($3\pi/2$), while the higher-energy part is nearly identical, we see a large difference in the lower-energy part, indicating the interference between the p-wave packets excited by the first and second pulses. This can be understood as follows. The wave

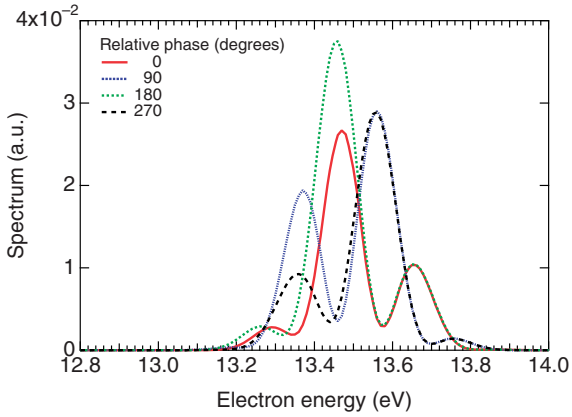

Figure 10. Two-photon ionization electron energy spectra by the double pulse with $T = 10$ fs and $\hbar\omega = 13.55$ eV with various relative phases ϕ_{rel} at $\tau = 378$ fs. The relative phase is controlled by varying the delay between 1237 and 1238 optical cycles. (The color version of this figure is included in the online version of the journal.)

packet generated by the first pulse is widely spread (Figure 8) and has a broad spectrum extending to the continuum (Figure 4). Only the part near the nucleus can interact with the second pulse and interfere with the wave packet excited by the second pulse. The inner part consists of the bound, lower energy part of the spectrum. As a consequence, it is mainly the low-energy part of the wave packet that is affected by the interference effect. This also indicates that, in spite of the rapid disintegration of the wave packet, its evolution itself is coherent.

6. Conclusions

Using numerical simulations based on the time-dependent Schrödinger equation, we have investigated two-photon ionization of a hydrogen atom by VUV pulses in the ultrashort pulse regime ($T \leq 10$ fs). The TPI is called stepwise when it proceeds via bound levels, well separated from the continuum. On the other hand, there are two different classes of direct TPI: a purely direct process with no real intermediate states involved, and a process involving Rydberg or continuum states as an intermediate level whose escaping time is very short. The presence of an intermediate resonant level, even bound, alone is not sufficient for the TPI to be stepwise.

Even for a wavelength corresponding to direct TPI in the long pulse limit, ionization becomes stepwise when the pulse is shorter than ca. 1 fs. This is due to the fact that spectral broadening of the pulse leads to resonant excitation of discrete bound levels. The relative population of different level strongly depends on pulse width. Hence, the dependence of the yield on pulse width is not quadratic, as is expected for stepwise processes in general. Moreover, the electron energy spectrum is not only broadened but also significantly red-shifted.

Unlike the Rydberg wave packet formed by a longer pulse, the wave packet generated by an ultrashort laser pulse rapidly disintegrates into several parts, due to its broad spectrum spanning from low-lying levels to the continuum. Nevertheless, the bound parts come back to the nucleus in fragments, and, especially, at early stages, each part returns in the Kepler orbit time corresponding to each central principal quantum number. If the second pulse coincides with the return, that part of the wave packet can be further ionized. The interference effect is more prominent for bound, lower-energy components of the wave packet, which manifests itself in the double-pulse TPI electron energy spectrum.

Acknowledgements

K.L. Ishikawa sincerely acknowledges financial support from the Ministry of Education, Culture, Sports, Science and Technology of Japan Grant Nos. 15035203, 15740252, and 19686006, and also a grant from Research Foundation for Opto-Science and Technology. This work was supported in part by the Precursory Research for Embryonic Science and Technology (PRESTO) program of the Japan Science and Technology Agency (JST), and also by the Advanced Photon Science Alliance (APSA) project.

References

[1] McPherson, A.; Gibson, G.; Jara, H.; Johann, U.; Luk, T.S.; McIntyre, I.A.; Boyer, K.; Rhodes, C.K. *J. Opt. Soc. Am. B* **1987,** *4,* 595–601.
[2] Ferray, M.; L'Huillier, A.; Li, X.F.; Lompré, L.A.; Mainfray, G.; Manus, C. *J. Phys. B* **1988,** *21,* L31–L35.
[3] L'Huillier, A.; Balcou, P. *Phys. Rev. Lett.* **1993,** *70,* 774–777.
[4] Macklin, J.J.; Kmetec, J.D.; Gordon, C.L. *Phys. Rev. Lett.* **1993,** *70,* 766–769.
[5] Goulielmakis, E.; Schultze, M.; Hofstetter, M.; Yakovlev, V.S.; Gagnon, J.; Uiberacker, M.; Aquila, A.L.; Gullikson, E.M.; Attwood, D.T.; Kienberger, R.; Krausz, F.; Kleineberg, U. *Science* **2008,** *320,* 1614–1617.
[6] Drescher, M.; Hentschel, M.; Kienberger, R.; Drescher, M.; Hentschel, M.; Kienberger, R.; Uiberacker, M.; Yakovlev, V.; Scrinzi, A.; Westerwalbesloh, T.; Kleineberg, U.; Heinzmann, U.; Krausz, F. *Nature* **2002,** *419,* 803–807.
[7] Baltuska, A.; Udem, T.; Uiberacker, M.; Hentschel, M.; Goulielmakis, E.; Gohle, C.; Holzwarth, R.; Yakovlev, V.; Scrinzi, A.; Hänsch, T.W.; Krausz, F. *Nature* **2003,** *421,* 611–615.
[8] Kienberger, R.; Goulielmakis, E.; Uiberacker, M.; Baltuska, A.; Yakovlev, V.; Bammer, F.; Scrinzi, A.;

Westerwalbesloh, T.; Kleineberg, U.; Heinzmann, U.; Drescher, M.; Krausz, F. *Nature* **2004,** *427,* 817–821.
[9] Krausz, F.; Ivanov, M. *Rev. Mod. Phys.* **2009,** *81,* 163–234.
[10] Goulielmakis, E.; Uiberacker, M.; Kienberger, R.; Baltuska, A.; Yakovlev, V.; Scrinzi, A.; Westerwalbesloh, T.; Kleineberg, U.; Heinzmann, U.; Drescher, M.; Krausz, F. *Science* **2004,** *305,* 1267–1269.
[11] Tamaki, Y.; Itatani, J.; Nagata, Y.; Obara, M.; Midorikawa, K. *Phys. Rev. Lett.* **1999,** *82,* 1422–1425.
[12] Takahashi, E.; Nabekawa, Y.; Otsuka, T.; Obara, M.; Midorikawa, K. *Phys. Rev. A* **2002,** *66,* 021802.
[13] Takahashi, E.; Nabekawa, Y.; Midorikawa, K. *Opt. Lett.* **2002,** *27,* 1920–1922.
[14] Takahashi, E.J.; Nabekawa, Y.; Midorikawa, K. *Appl. Phys. Lett.* **2004,** *84,* 4–6.
[15] Hergott, J.F.; Kovacev, M.; Merdji, H.; Hubert, C.; Mairesse, Y.; Jean, E.; Breger, P.; Agostini, P.; Carré, B.; Salières, P. *Phys. Rev. A* **2002,** *66,* 021801.
[16] Yoshitomi, D.; Shimizu, T.; Sekikawa, T.; Watanabe, S. *Opt. Lett.* **2002,** *27,* 2170–2172.
[17] Mashiko, H.; Suda, A.; Midorikawa, K. *Opt. Lett.* **2004,** *29,* 1927–1929.
[18] Sekikawa, T.; Kosuge, A.; Kanai, T.; Watanabe, S. *Nature* **2004,** *432,* 605–608.
[19] Hasegawa, H.; Takahashi, E.J.; Nabekawa, Y.; Ishikawa, K.L.; Midorikawa, K. *Phys. Rev. A* **2005,** *71,* 023407.
[20] Ishikawa, K. *Phys. Rev. Lett.* **2003,** *91,* 043002.
[21] Ishikawa, K.L. *Appl. Phys. B* **2004,** *78,* 855–858.
[22] Ishikawa, K.L. *Phys. Rev. A* **2004,** *70,* 013412.
[23] Nabekawa, Y.; Hasegawa, H.; Takahashi, E.J.; Midorikawa, K. *Phys. Rev. Lett.* **2005,** *94,* 043001.
[24] Parker, J.S.; Moore, L.R.; Meharg, K.J.; Dundas, D.; Taylor, K.T. *J. Phys. B* **2001,** *34,* L69–L78.
[25] Laulan, S.; Bachau, H. *Phys. Rev. A* **2003,** *68,* 013409.
[26] Ishikawa, K.L.; Midorikawa, K. *Phys. Rev. A* **2005,** *72,* 013407.
[27] Barna, I.F.; Wang, J.; Burgdörfer, J. *Phys. Rev. A* **2006,** *73,* 023402.
[28] Foumouo, E.; Laulan, S.; Piraux, B.; Bachau, H. *J. Phys. B* **2006,** *39,* S427–S435.
[29] Palacios, A.; McCurdy, C.W.; Rescigno, T.N. *Phys. Rev. A* **2007,** *76,* 043420.
[30] Palacios, A.; Rescigno, T.N.; McCurdy, C.W. *Phys. Rev. A* **2008,** *77,* 032716.
[31] Palacios, A.; Rescigno, T.N.; McCurdy, C.W. *Phys. Rev. A* **2009,** *79,* 033402.
[32] Feist, J.; Pazourek, R.; Nagele, S.; Persson, E.; Schneider, B.I.; Collins, L.A.; Burgdörfer, J. *J. Phys. B* **2009,** *42,* 134014.
[33] Feist, J.; Nagele, S.; Pazourek, R.; Persson, E.; Schneider, B.I.; Collins, L.A.; Burgdörfer, J. *Phys. Rev. Lett.* **2009,** *103,* 063002.
[34] Chan, F.T.; Tang, C.L. *Phys. Rev.* **1969,** *185,* 42–44.
[35] Jayadevan, A.P.; Thayyullathil, R.B. *J. Phys. B* **2001,** *34,* 699–703, and references therein.
[36] Zernik, W *Phys. Rev.* **1964,** *135,* A51–A57.
[37] Bebb, H.B.; Gold, A. *Phys. Rev.* **1966,** *143,* 1–24.
[38] Gontier, Y.; Trahin, M. *Phys. Rev.* **1968,** *172,* 83–87.
[39] Laplanche, G.; Durrieu, A.; Flank, Y.; Jaouen, M.; Rachman, A. *J. Phys. B* **1976,** *9,* 1263–1277.
[40] Ishikawa, K.; Midorikawa, K. *Phys. Rev. A* **2002,** *65,* 043405.
[41] Kulander, K.C.; Schafer, K.J.; Krause, J.L. In *Atoms in Intense Laser Fields*; Gavrila, M., Ed.; Academic Press: New York, 1992; pp 247–300.
[42] Alber, G.; Ritsch, H.; Zoller, P. *Phys. Rev. A* **1986,** *34,* 1058–1064.
[43] Noordam, L.D.; Duncan, D.I.; Gallagher, T.F. Ramsey *Phys. Rev. A* **1992,** *45,* 4734–4737.
[44] Jones, R.R.; Raman, C.S.; Schumacher, D.W.; Bucksbaum, P.H. *Phys. Rev. Lett.* **1993,** *71,* 2575–2578.
[45] Parker, J.; Stroud, C.R. *Phys. Rev. Lett.* **1986,** *56,* 716–719.
[46] Krause, J.L.; Schafer, K.J.; Kulander, K.C. *Phys. Rev. A* **1992,** *45,* 4998–5010.
[47] Schafer, K. *Computer Phys. Comms.* **1991,** *63,* 427–434.
[48] Fano, U.; Cooper, J.W. *Rev. Mod. Phys.* **1968,** *40,* 441–507.
[49] ten Wolde, A.; Noordam, L.D.; Lagendijk, A.; van Linden van den Heuvell, H.B. *Phys. Rev. Lett.* **1988,** *61,* 2099–2101.
[50] Lindner, F.; Schätzel, M.G.; Walther, H.; Baltuška, A.; Goulielmakis, E.; Krausz, F.; Milošević, D.B.; Bauer, D.; Becker, W.; Paulus, G.G. *Phys. Rev. Lett.* **2005,** *95,* 040401.
[51] Ishikawa, K.L. *Phys. Rev. A* **2006,** *74* (2), 023806.